Partial Safety Factor for the Design Strength Prediction of Naturally Corroded Prestressing Strands

Lorenzo Franceschini
PhD Student, Dept. of Architecture and Civil Engineering, University of Parma, Parma, Italy

Wouter Botte
Post Doctoral Researcher, Dept. of Structural Engineering and Building materials, Ghent University, Ghent, Belgium

Robby Caspeele
Professor, Dept. of Structural Engineering and Building materials, Ghent University, Ghent, Belgium

Beatrice Belletti
Professor, Dept. of Architecture and Civil Engineering, University of Parma, Parma, Italy

Francesco Tondolo
Associate Professor, Dept. of Structural, Geotechnical and Building Engineering, Politecnico di Torino, Turin, Italy

Javier Sanchez
Senior Research Engineer, Institute Eduardo Torroja of Construction Science., Madrid, Spain

ABSTRACT: Existing reinforced and prestressed concrete structures are often affected by corrosion triggering high annual maintenance costs and impairing their safety, durability and serviceability. Although scientific studies have been devoted to the development of reliable methods for determining the residual resistance of such structures, the daily engineering practice is hindered by the lack of simplified models that consider all relevant uncertainties. The present contribution defines a partial factor for the calculation of the design tensile strength of corroded prestressing strands. To this aim, uncertainties related to material properties and geometry are defined according to the latest draft of the future *fib* Model Code 2020 prescriptions, whereas the model uncertainty is evaluated for a novel model, which derives the tensile strength based on the maximum penetration depth of the most corroded wire. First, the spatial variability of pitting corrosion of several naturally corroded prestressing strands is investigated by means of a 3D scanning technique. Second, a procedure for the estimation of the maximum penetration depth of a corroded prestressing strand is introduced. Finally, a simplified stress-strain relationship, named SCPS-model, is adopted for the prediction of the residual ultimate strength of prestressing strands. The obtained outcomes provide a useful tool for the assessment of existing prestressed concrete structures subjected to corrosion deterioration in everyday engineering practice.

1. INTRODUCTION

Corrosion of steel reinforcements is nowadays considered as one of the leading causes of the durability and performance reduction of existing Reinforced Concrete (RC) and Prestressed Concrete (PC) structures, Angst (2018). Furthermore, most of the existing structures have already exceeded their design service life and show evident signs of deterioration.

Although scientific studies have been focused to the development of reliable methods for determining the residual structural capacity of corroded existing structures, the daily engineering practice is hindered by the lack of simplified models that consider all relevant uncertainties. All

engineering models are characterized by a certain level of uncertainty because of the variability of material and geometrical properties as well as the calculation model itself. As pointed out by Blomfors et at. (2019) in the case of a probabilistic bond model for the estimation of the anchorage capacity of corroded rebars, the application of simplified models for the assessment of existing structures must be accomplished with a sufficient margin of safety, especially if the interested structures exhibit corrosion damage. In addition, the assessment of existing structures often differs from the design of new ones because of the different importance of the involved variables. Caspeele et al. (2013) proposed a Design Value Method (DVM) for adjusted partial safety factors for the evaluation of existing structures allowing to account for different variabilities of the basic variables, a different target safety level, expressed by the reliability index β_{target}, and a different reference period compared to the values usually adopted for design. Although DVM is already considered in Codes and Guidelines, such as the *fib* Bulletin 80 (2016), the evaluation of Partial Safety Factors (PSF) for existing RC and PC structures do currently not take into account reduced material characteristics. Therefore, the present work proposes a PSF for the prediction of the design tensile strength of corroded prestressing strands. To this end, uncertainties related to material properties, geometry and failure mode are defined according to the latest draft of the future *fib* Model Code 2020 prescriptions. Moreover, the model uncertainty associated with the SCPS-model proposed by Franceschini et al. (2022a), which predicts the residual mechanical properties of a corroded strand as a function of the maximum penetration depth of the most corroded wire, is defined based on the spatial variability of pitting corrosion in several naturally corroded prestressing strands.

2. METHODOLOGY

2.1.1. Partial factor for the assessment of corroded prestressing strands

The proposed PSF $\gamma_{m,corr}$ is defined by Eq. (1):

$$\gamma_{m,corr} = \frac{\exp(-1.645 V_s)}{\mu_{\mathrm{mod}} \mu_a \mu_{\vartheta R} \cdot \exp\left(-\alpha \beta_{target} \sqrt{V_{\mathrm{mod}}^2 + V_a^2 + V_s^2 + V_{\vartheta R}^2}\right)} \quad (1)$$

where:

- V_s is the coefficient of variation (COV) of uncorroded strength of prestressing steel, which is assumed to be equal to 0.025 according to JCSS (2001) recommendations.
- α is the sensitivity factor, assumed equal to 0.7 for a 1-year reference period according to the latest draft of the future Model Code 2020, Caspeele (2021).
- β_{target} is the annual target reliability index adopted from JCSS (2001) and ISO 2394 (2015) provisions, considering the assessment of a structure characterized by a consequence class CC2 and a large relative cost of safety measures, i.e. β_{target} equal to 3.3 (Table 1).

Table 1: β_{target} based on economic optimization.

Cost of safety measures	*Consequence class*		
	CC1	*CC2*	*CC3*
Large (A)	*3.1*	***3.3***	*3.7*
Normal (B)	*3.7*	*4.2*	*4.4*
Small (C)	*4.2*	*4.4*	*4.7*

- μ_a and V_a are, respectively, the mean and COV related to geometrical properties. In case of existing concrete structures, the latter uncertainty should be evaluated by means of in-situ analysis. However, in the lack of available measurements, the latest draft of the future Model Code 2020 proposes μ_a and V_a values equal to 1.0 and 0.01.
- $\mu_{\theta R}$ and $V_{\theta R}$ are, respectively, the mean value and COV of the resistance model uncertainty. The latest draft of the future Model Code 2020 distinguishes between failure modes associated with bending (reinforcement properties are mostly dominating) or crushing of columns (concrete compressive strength is dominating) to provide indicative values of resistance model uncertainty. Nevertheless, the suggested values are for non-deteriorating RC members, while no recommendations are

provided for existing PC members subjected to chloride-induced corrosion. Considering the absence of specific provisions, $\mu_{\theta R}$ and $V_{\theta R}$ are assumed to be equal to 1.09 and 0.045, valid for members failing in bending. Therefore, the derived PSF should be used in the assessment of PC members adopting an analytical model for the verification of its bending resistance. Future research efforts should be devoted to the specific evaluation of the resistance model uncertainty of corroded PC members.

- μ_{mod} and V_{mod} represent the mean value and COV related to the analytical predictions of the residual ultimate strength of corroded strands obtained by using the SCPS-model (see Section 2.1.2). These latter values are strongly related to corrosion effects and their evaluation and quantification are thoroughly analyzed in the present work.

It is worth noting that a PSF value, $\gamma_{m,uncorr}$, of $0.994 \approx 1$ is estimated for the uncorroded scenario by substituting the assumed uncertainty values in Eq. (2) and by initially neglecting the corrosion effects associated with the SCPS-model uncertainty, i.e. μ_{mod} and V_{mod} factors.

$$\gamma_{m,uncorr} = \frac{\exp(-1.645V_s)}{\mu_a \mu_{\vartheta R} \cdot \exp\left(-\alpha\beta_{target}\sqrt{V_a^2 + V_s^2 + V_{\vartheta R}^2}\right)} = \frac{\exp(-1.645 \cdot 0.025)}{1.0 \cdot 1.09 \cdot \exp\left(-0.7 \cdot 3.3\sqrt{0.01^2 + 0.025^2 + 0.045^2}\right)} = 0.994 \quad (2)$$

2.1.2. The SCPS-model

To investigate the residual mechanical behaviour of corroded prestressing strands, several strands were retrieved from naturally corroded PC beams. Second, 3D models of uncorroded and corroded samples were obtained by using a structured light 3D scanner. The pitting morphology was then investigated by superimposing the uncorroded and corroded 3D models using the GOM Inspect software, as shown in Figure 1. Finally, tensile tests were conducted at the MastrLab Laboratory of the Politecnico of Turin. The experimental results in terms of ultimate corroded strength, $f_{pu,corr,exp,i}$, are reported in Table 2. Following tensile testing, the experimental force-strain relationships of the analyzed samples were evaluated by combining the load recorded during the displacement-control procedure with the strain field evolution obtained from the Digital Image Correlation (DIC) analysis.

By analyzing the experimental data, a simplified constitutive, named SCPS-model, was proposed for the prediction of the residual stress-strain response of corroded strands. The main features of the SCPS-model are briefly outlined hereafter, while more details on the SCPS-model and pitting morphology can be found in Franceschini et al. (2022a) and Vecchi et al. (2021), respectively.

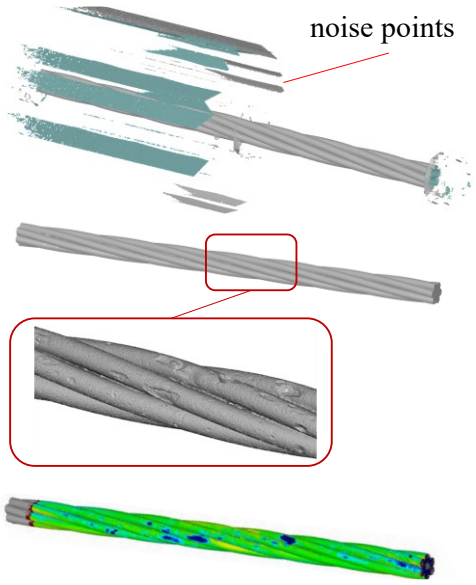

Figure 1: Focus on 3D models superimposition.

The SCPS-model has been designed based on the equivalent spring material model. The latter approach reproduces the overall sectional response of a corroded strand as the sum of wire contributions, which are assumed as springs working in parallel. In this context, the SCPS-model is intended for the daily engineering practice and conceived on a single input parameter that is the maximum penetration depth of the most corroded wire, denoted as $P_{max,sectional,i}$. As a result, the SCPS-model has been developed to be independent from: (i) the pit type

morphology classification, and (ii) the evaluation of corrosion parameters such as the mass loss, η, of a corroded strand or the cross-sectional loss, μ, of corroded wires. The model adopts a single bi-linear decay law for the ultimate strain and estimates a sectional average penetration depth for the remaining external wires, $P_{av,sectional,i}$, as a function of the $P_{max,sectional,i}$ value via the adoption of a transversal pitting factor, Ω_i, defined in Franceschini et al. (2022b). The corroded area of wires is considered for the final prediction of the stress-strain response of the overall strand. For this purpose, a bi-linear decay law for the evaluation of the residual cross-sectional area of the wire has been also introduced.

Further relevant assumptions of the SCPS-model are as follow:

- The conventional failure of the entire strand is assumed to occur in case of the first rupture of the most corroded wire. Nevertheless, the subsequent simultaneous failure of the remaining external wires, characterized by the same $P_{av,sectional,i}$, can be predicted.
- The SCPS-model assumes a tri-linear relationship for representing the stress-strain behaviour of uncorroded and low corroded wires. The tri-linear trend consists of: (a) an elastic phase ranging from (0; 0) to ($\varepsilon_{pp,0}$;$f_{pp,0}$), a yielding phase from ($\varepsilon_{pp,0}$;$f_{pp,0}$) to ($\varepsilon_{py,0}$;$f_{py,0}$) and a hardening phase from ($\varepsilon_{py,0}$; $f_{py,0}$) to ($\varepsilon_{pu,0}$;$f_{pu,0}$), as shown in Figure 2. By contrast, for intermediate and highly corroded wires the tri-linear trend reduces to a bi-linear or even a linear trend as a function of the normalized value of maximum penetration depth, $P_{max,sectional,i}/r_{outer}$, of the analyzed wire, where r_{outer} represents the uncorroded radius of the external wires.
- The ultimate corroded strength, $f_{pu,corr,an,i}$, is evaluated in correspondence to the ultimate corroded strain, $\varepsilon_{pu,corr,an}$. To this end, the SCPS-model estimates the ultimate corroded strain decay through a bi-linear relationship expressed as a function of $P_{max,sectional,i}/r_{outer}$. According to the SCPS-model assumptions, the stress-strain relationship of corroded and uncorroded wires is equivalent; the only difference lies in the cut-off point, established at the achievement of the previously determined ultimate corroded strain, $\varepsilon_{pu,corr,an}$. For low corroded wires ($P_{max,sectional,i}/r_{outer}$ < 0.33), a tri-linear stress-strain relationship with a reduced hardening phase is adopted. Conversely, a bi-linear relationship is assumed for intermediate corroded wires (0.33 < $P_{max,sectional,i}/r_{outer}$ < 0.86); whereas, for the highly corroded ones (0.86 < $P_{max,sectional,i}/r_{outer}$), a linear relationship is adopted.

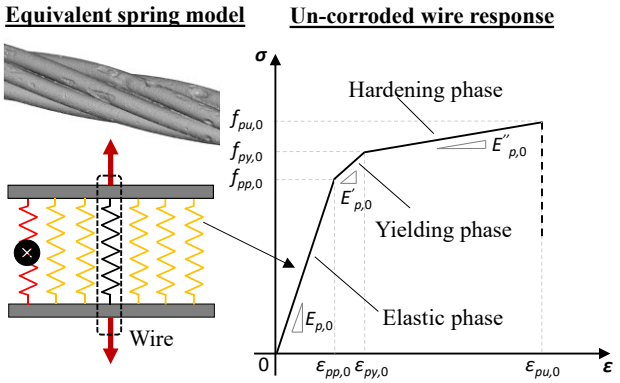

Figure 2: Equivalent spring material model and stress-strain relationship for the uncorroded wire.

To summarize, once the $P_{max,sectional,i}$ value is known, the $P_{av,sectional,i}$ value is first determined. Second, the ultimate corroded strain, $\varepsilon_{pu,corr,an}$, of each wire is estimated by adopting a bi-linear decay law. Then, the wires' ultimate corroded strengths are estimated. Finally, the $f_{pu,corr,an,i}$ of the entire strand is predicted through the adoption of the equivalent spring material model by considering the wires' residual cross-sectional area. The expressions for the prediction of the ultimate corroded strength are pointed out in the flowchart shown in Figure 3.

Although the SCPS-model proved to be a simplified but accurate tool for the prediction of the residual mechanical properties of a corroded strand, see Franceschini et al. (2022a), several uncertainties are inherently connected to the proposed model, such as: (a) the uncertainty related to the maximum penetration depth

measurement, (b) the uncertainty related to the ultimate corroded strain and strength predictions, and (c) the uncertainty related to the estimation of the average penetration depth attributed to the remaining external wires.

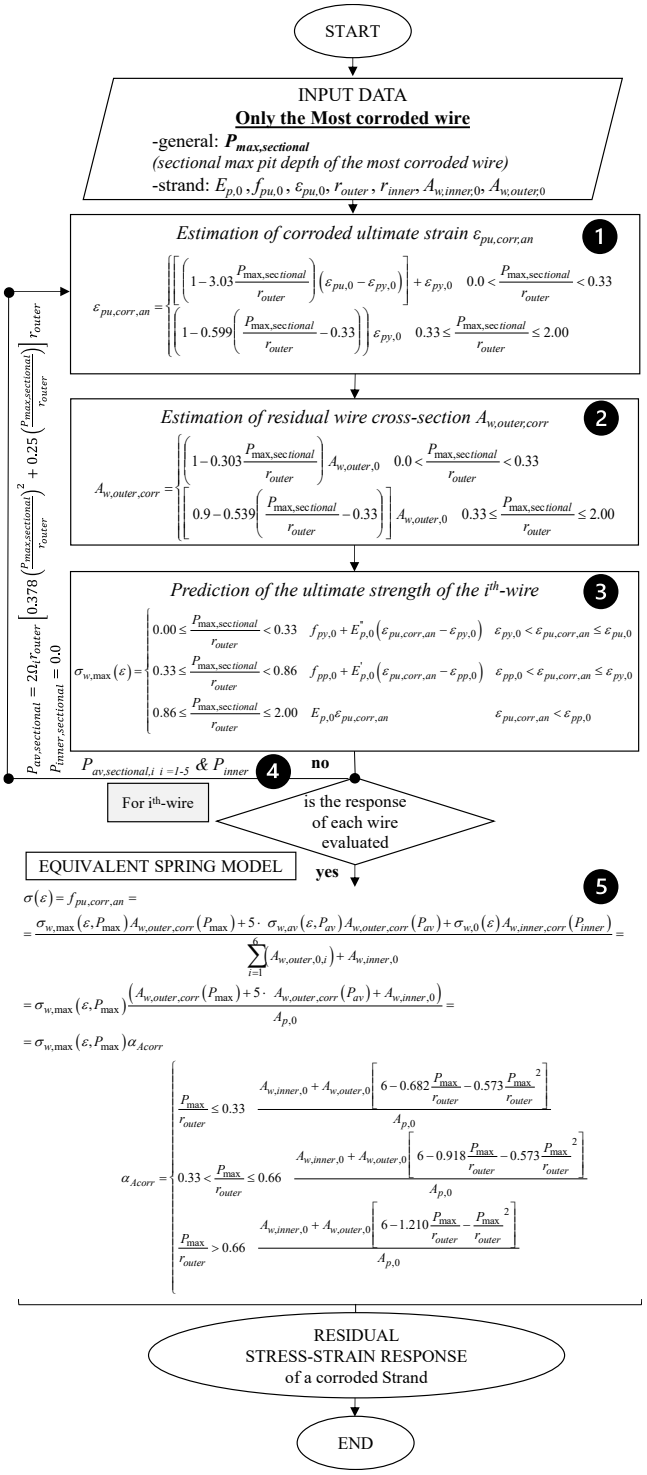

Figure 3: SCPS-model flowchart.

These uncertainties should be accounted for in the new PSF, $\gamma_{m,corr}$, which is evaluated to estimate the design tensile strength of a corroded prestressing strand, $f_{pu,corr,des,i}$, according to Eq. (3):

$$f_{pu,corr,des,i} = \frac{f_{pu,corr,an,i}}{\gamma_{m,corr}} \quad (3)$$

3. RESULTS

Before deriving the characteristics μ_{mod} and V_{mod} of the model uncertainty of the SCPS-model in section 3.2, a procedure to derive the maximum penetration depth based on individual penetration depth measurements is proposed in section 3.1.

3.1. Maximum penetration depth evaluation

Since the SCPS-model relies on the maximum penetration depth, first, a simplified procedure was developed to estimate the latter based on several individual pit depth measurements.

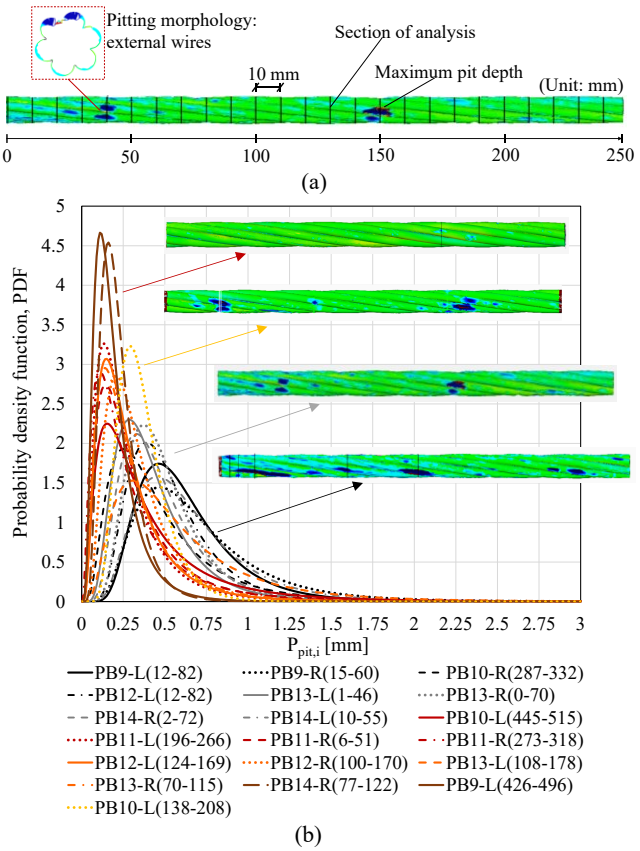

Figure 4: Pitting morphology analysis: (a) sectional analysis, and (b) lognormal distributions of corroded strands variability in terms of penetration depth for different corrosion levels.

To this end, the number of pits, n_{pits}, and the related penetration depths, P_x, were measured by conducting a sectional analysis every 10 mm, as shown in Figure 4(a). Next, according to the studies conducted by Wang et al. (2020), a lognormal distribution was adopted to fit the measured penetration depths of each sample, as expressed in Eq. (4) and shown in Figure 4(b):

$$f_X(x) = \frac{1}{\sqrt{2\pi}\zeta_x x}\exp\left[-\frac{1}{2}\left(\frac{\ln x - \lambda_x}{\zeta_x}\right)^2\right] \quad (4)$$

The parameters $\lambda_{x,i}$ and $\zeta_{x,i}$ are reported in Table 2.

Afterwards, the fractile value $\xi_{max,i}$ of the measured maximum penetration depth $P_{max,sectional,i}$ was calculated. It is assumed that the maximum penetration depth can be estimated in a simplified way as this fractile of the distribution of the individual penetration depth measurements (cfr. Eq. (5)).

Table 2: Tensile test results and lognormal distribution parameters for each analyzed strand.

Sample ID	$f_{pu,corr,exp,i}$ [MPa]	$\lambda_{x,i}$ [-]	$\zeta_{x,i}$ [-]
L_{scan} =250 *mm*			
PB9-R(15-60)	*1082.0*	*-0.49*	*0.5148*
PB10-R(287-332)	*766.0*	*-0.94*	*0.6590*
PB11-R(6-51)	*1642.0*	*-1.36*	*0.7599*
PB11-R(273-318)	*1387.0*	*-1.47*	*0.8670*
PB12-L(124-169)	*1491.0*	*-1.43*	*0.6926*
PB13-L(1-46)	*1562.0*	*-0.97*	*0.5275*
PB13-R(70-115)	*1562.0*	*-1.43*	*0.7381*
PB14-L(10-55)	*1239.0*	*-0.55*	*0.4915*
PB14-R(77-122)	*-*	*-1.60*	*0.4884*
L_{scan} =500 *mm*			
PB9-L(12-82)	*1186.9*	*-0.57*	*0.4470*
PB9-L(426-496)	*1799.0*	*-1.79*	*0.6223*
PB10-L(138-208)	*1667.0*	*-1.08*	*0.3911*
PB10-L(445-515)	*944.0*	*-1.20*	*0.8242*
PB11-L(196-266)	*1516.0*	*-1.51*	*0.7089*
PB12-L(12-82)	*1185.0*	*-0.73*	*0.4594*
PB12-R(100-170)	*1492.0*	*-1.24*	*0.5716*
PB13-R(0-70)	*1381.0*	*-0.80*	*0.4363*
PB13-L(108-178)	*861.0*	*-0.72*	*0.6735*
PB14-R(2-72)	*1452.0*	*-0.86*	*0.5053*

Since the investigated corroded prestressing strands were characterized by different scanned lengths, L_{scan}, of 250 mm and 500 mm, the proposed procedure was conducted by distinguishing two groups of samples. Table 3 reports the obtained fractile values, $\xi_{max,i}$.

Table 3: Estimation of the maximum penetration depth and residual / design strength prediction.

Sample ID abbreviated	$\xi_{max,i}$ [-]	$\mu_{Pmax,i}$ [mm]	$f_{pu,corr,an,i}$ [MPa]	$f_{pu,corr,des,i}$ [MPa]
L_{scan} =250 *mm*				
9 (15-60)	*0.998*	*1.89*	*1037.2*	*791.7*
10 (287-332)	*0.999*	*1.65*	*1171.5*	*894.2*
11 (6-51)	*0.960*	*1.35*	*1324.0*	*1010.6*
11 (273-318)	*0.975*	*1.54*	*1230.8*	*939.4*
12 (124-169)	*0.991*	*1.08*	*1439.3*	*1098.6*
13 (1-46)	*0.995*	*1.20*	*1389.7*	*1060.7*
13 (70-115)	*0.980*	*1.21*	*1385.5*	*1057.5*
14 (10-55)	*0.997*	*1.70*	*1147.6*	*875.9*
14 (77-122)	*0.978*	*0.59*	*1656.1*	*-*
L_{scan} =500 *mm*				
9 (12-82)	*0.993*	*1.38*	*1312.6*	*1001.9*
9 (426-496)	*0.933*	*0.57*	*1662.5*	*1268.9*
10 (138-208)	*0.920*	*0.74*	*1591.3*	*1214.6*
10 (445-515)	*0.994*	*1.56*	*1218.3*	*929.9*
11 (196-266)	*0.995*	*0.91*	*1517.3*	*1158.1*
12 (12-82)	*0.994*	*1.20*	*1390.5*	*1061.3*
12 (100-170)	*0.985*	*0.90*	*1521.7*	*1161.5*
13 (0-70)	*0.995*	*1.07*	*1445.4*	*1103.2*
13 (108-178)	*0.976*	*1.86*	*1058.9*	*808.2*
14 (2-72)	*0.982*	*1.16*	*1408.3*	*1074.9*

The mean value, $\mu_{\xi max}$, and the standard deviation, $\sigma_{\xi max}$, of the fractile values, $\xi_{max,i}$, were then calculated for the two groups. The latter parameters are respectively equal to 0.986 and 0.0134 for the group with L_{scan} of 250 mm and equal to 0.977 and 0.0274 for the group with L_{scan} of 500 mm. Finally, the relationship between the mean of the maximum penetration depth, $\mu_{Pmax,i}$, and the parameters $\lambda_{x,i}$ and $\zeta_{x,i}$ related to the measured pits is proposed through Eq. (5):

$$\mu_{P_{\max,i}} = \exp\left(\lambda_{x,i} + \zeta_{x,i}\Phi^{-1}\left(\mu_{\xi_{\max}}\right)\right) \quad (5)$$

where Φ^{-1} is the inverse standard normal distribution function. The estimated $\mu_{Pmax,i}$ represents the maximum penetration depth, $P_{max,sectional,i}$, to be adopted as the input parameter for the prediction of the ultimate corroded

strength, $f_{pu,corr,an,i}$, through the adoption of the SCPS-model. The predicted $\mu_{Pmax,i}$ and $f_{pu,corr,an,i}$ are reported in Table 3.

3.2. SCPS-model uncertainty quantification

As extensively discussed by Engen et al. (2017), the probability distribution of the model uncertainty is generally unknown; however, it can be represented as a lognormally distributed random variable as suggested by the EN1990 (2015). This latter distribution was also selected based on the investigated variable fitting showed by the quantile plot reported in Figure 5.

According to Annex D of EN1990, once the $P_{max,sectional,i}$ values were evaluated, the SCPS-model uncertainty characteristics, denoted as μ_{mod} and V_{mod} in Eq. (1), can be calculated based on the natural logarithm of the parameter δ_i (denoted with Δ_i), which represent the error term associated with each experimental value $f_{pu,corr,exp,i}$. The δ_i values were first evaluated through Eq.(6):

$$\delta_i = \frac{f_{pu,corr,\exp,i}}{b \cdot f_{pu,corr,an,i}} \tag{6}$$

where b – calculated in Eq. (7) – stands for the "Least Squares" best-fit of the slope correlating the theoretical and experimental values of the investigated variable, as shown in Figure 6.

$$b = \frac{\sum f_{pu,corr,\exp,i} f_{pu,corr,an,i}}{\sum f_{pu,corr,an,i}^2} = 1.0037 \tag{7}$$

Second, the mean value ($\bar{\Delta}$), the variance (s_Δ^2), the standard deviation (s_Δ), and the COV (V_δ) of the term Δ were estimated according to Eqs. (8) to (10), where n is the number of available observations. It is worth noting that $\bar{\Delta}$, s_Δ, and V_δ correspond to the mean value (μ_{ln}), the standard deviation (σ_{ln}), and the COV (V_{ln}) of the analyzed lognormal distribution function, respectively. Afterwards, considering the relationships between lognormal and normal distribution function parameters – Eqs. (11) and (12) – the mean value, μ_{mod}, and the standard deviation, σ_{mod}, of the SCPS-model uncertainty were calculated, resulting in the values 0.9905 and 0.1580, respectively; whereas the COV, V_{mod}, of 0.1595 was estimated as the ratio between σ_{mod} and μ_{mod}.

$$\bar{\Delta} = \frac{1}{n}\sum_1^n \Delta_i = -0.0221 = \mu_{\ln} \tag{8}$$

$$s_\Delta^2 = \frac{1}{n-1}\sum_{i=1}^n \left(\Delta_i - \bar{\Delta}\right)^2 = 0.025 \tag{9}$$

$$s_\Delta = \sqrt{s_\Delta^2} = 0.1585 = \sigma_{\ln}$$

$$V_\delta = \sqrt{\exp\left(s_\Delta^2\right) - 1} = 0.1595 = V_{\ln} \tag{10}$$

$$\mu_{\ln} = \ln \mu_{\mathrm{mod}} - \frac{1}{2}\ln\left(V_{\mathrm{mod}}{}^2 + 1\right) \tag{11}$$

$$\sigma_{\ln} = \sqrt{\ln\left(V_{\mathrm{mod}}^2 + 1\right)} \tag{12}$$

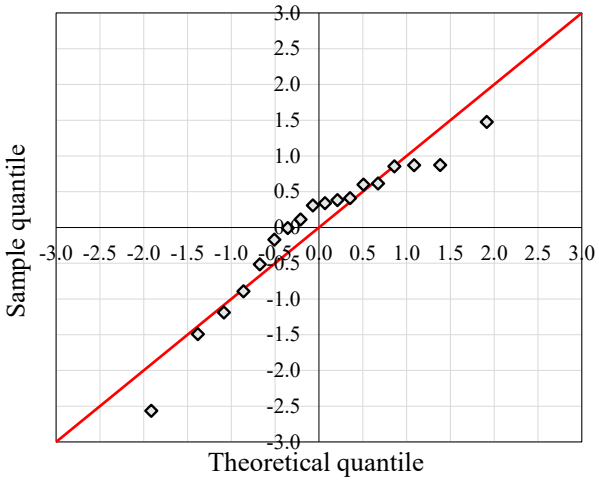

Figure 5: Quantile plot by considering Δ_i values.

In addition, to verify the selected distribution type, the Shapiro-Wilk test of normality was performed and compared to a 5% level of significance, Shapiro & Wilk (1965). The test, conducted on $\Delta_i = \ln(\delta_i)$ values provided a Shapiro-Wilk test statistic for normality, W, and a related P-value equal to 0.9069 and 0.0715, respectively. Based on the obtained results, the test is successful if compared to a 5% level of significance, which means that the Δ_i observations can be reasonably treated as a lognormally distributed random variable. Finally, the proposed PSF, $\gamma_{m,corr}$, of 1.31 was determined by replacing the estimated μ_{mod} and V_{mod} values in Eq. (13).

$$\gamma_{m,corr} = \frac{\exp(-1.645 \cdot 0.025^2)}{0.9905 \cdot 1.0 \cdot 1.09 \cdot \exp\left(-0.7 \cdot 3.3\sqrt{0.1595^2 + 0.01^2 + 0.025^2 + 0.045^2}\right)} = 1.31 \tag{13}$$

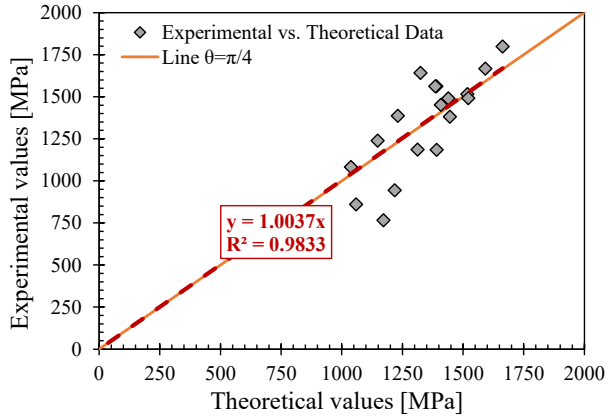

Figure 6: Theoretical vs Experimental outcomes.

For completeness, the estimated $f_{pu,corr,des,i}$ values are highlighted in Table 3.

4. CONCLUSIONS

The proposed PSF defines a simplified procedure for the prediction of the design ultimate strength of a corroded strand, by considering several uncertainties.

Although the estimated PSF, $\gamma_{m,corr}$, of 1.31 should be regarded as a valuable tool for daily engineering practice to be implemented in future Codes and Guidelines for the assessment of existing corroded PC members, its effectiveness requires further investigation. To improve the accuracy of the proposed $\gamma_{m,corr}$, additional experimental tests on corroded strands should be conducted to extend the available statistical population. Finally, it is worth noting that the proposed PSF is only valid in combination with the SCPS-model adoption, i.e. when the ultimate tensile strength is estimated via the proposed methodology. In the absence of portable 3D laser scanners, a pit depth gauge instrument can be used for pits' measurement during in-situ inspection.

5. ACKNOWLEDGEMENTS

The presented study is part of a program of activities funded by the Italian "Consiglio Superiore dei Lavori Pubblici".

6. REFERENCES

Angst, U. M. 2018. "Challenges and opportunities in corrosion of steel in concrete." *Mater. Struct. Constr.*, 51 (1): 1–20. Springer Netherlands.

Blomfors, M., O. Larsson Ivanov, D. Honfi, and M. Engen. 2019. "Partial safety factors for the anchorage capacity of corroded reinforcement bars in concrete." *Eng. Struct.*, 181: 579–588. Elsevier.

Caspeele, R. 2021. "Partial factor based assessment of existing concrete structures: new developments and applications." *Proc. fib CACRCS DAYS 2021 - Capacit. Assess. Corroded Reinf. Concr. Struct. Venue on-line 30th Nov.- 3rd Dec. 2021*, 3–6.

Caspeele, R., M. Sykora, D. L. Allaix, and R. Steenbergen. 2013. "The design value method and Adjusted Partial Factor Approach for existing structures." *Struct. Eng. Int. J. Int. Assoc. Bridg. Struct. Eng.*, 23 (4): 386–393.

CEB-fip. 2016. *fib Belletin 80: Partial factor methods for existing concrete structures*. Lousanne, Switzerland.

CEN. 2015. *Eurocode 0 - Basis of structural design*. Brussels, Belgium.

Engen, M., M. A. N. Hendriks, J. Köhler, J. A. Øverli, and E. Åldstedt. 2017. "A quantification of the modelling uncertainty of non-linear finite element analyses of large concrete structures." *Struct. Saf.*, 64: 1–8. Elsevier Ltd.

Franceschini, L., B. Belletti, F. Tondolo, and J. Sanchez. 2022a. "A simplified stress-strain relationship for the mechanical behaviour of corroded prestressing strands: the SCPS-model." *Struct. Concr.*

Franceschini, L., B. Belletti, F. Tondolo, and J. Sanchez. 2022b. "Study on the Probability Distribution of Pitting for Naturally Corroded Prestressing Strands Accounting for Surface Defects." *Buildings*, 12 (10).

ISO. 2015. *ISO 2394:2015: General principles on reliability for structures*. Geneva, Switzerland.

JCSS. 2001. *JCSS. Probabilistic Model Code - Part 3: Resistance Models*. Chapter 3.04: pp.1-7.

Shapiro, A. S. S., and M. B. Wilk. 1965. "An Analysis of Variance Test for Normality (Complete Samples)." *Biometrika*, 52 (3): 591–611.

Vecchi, F., L. Franceschini, F. Tondolo, B. Belletti, J. Sánchez Montero, and P. Minetola. 2021. "Corrosion morphology of prestressing steel strands in naturally corroded PC beams." *Constr. Build. Mater.*, 296.

Wang, L., T. Li, L. Dai, W. Chen, and K. Huang. 2020. "Corrosion morphology and mechanical behavior of corroded prestressing strands." *J. Adv. Concr. Technol.*, 18 (10): 545–557.